

# Analysis of lifting system of FAST feed receiver robot

Dong Sun<sup>ab</sup>, Xudong Yang<sup>\*a</sup>, Ligang Qiang<sup>c</sup>, Yong Zhang<sup>c</sup>

<sup>a</sup>School of Mechanical Engineering, Guizhou University, Guiyang, Guizhou, China; <sup>b</sup>College of Mechanical Engineering, Guizhou Institute of Technology, Guiyang, Guizhou, China; <sup>c</sup>Aerospace Jiangnan Group Co., Ltd., Guiyang, Guizhou, China

## ABSTRACT

This research mainly focuses on the analysis of the lifting system of the FAST receiver robot. The deformation will appear after loads are added to the spatial mechanism; and this will further affect the smooth operation of the mechanism. The finite element method is applied to the lifting system of the FAST feed receiver disassembly and handling robot; the stress and deformation distributions of the lifting system under rated working conditions can thus be analyzed and related results have also been obtained. The resultant results provide references for the actual performance of the lifting system. The results also reveal that the maximum deformation as well as the stress meet the predetermined requirements of the lifting system.

**Keywords:** FAST feed receiver robot, lifting system, stiffness, finite element analysis

## 1. INTRODUCTION

According to the requirements of safe disassembly and handling of the feed receiver of the Five-hundred-meter Aperture Spherical Telescope (FAST), especially the factors such as heavy workload of bolt disassembly and assembly, inconvenient handling of the feed cabin and low disassembly efficiency, a feed receiver disassembly and assembly robot system integrating positioning, disassembly, transportation and other functions is designed. Figure 1 shows the working condition of the robot; the robot is divided into the bearing part and the lifting part. The bearing part is mainly realized by the AGV (Automatic Guided Vehicle) trolley at the bottom of the device and the top bracket, and the lifting part is mainly realized by the contraction and opening of the spatial parallel mechanism. The workpiece is placed on the bracket above the parallel mechanism.

The lifting system is required to have good rigidity and small size and weight. Among the structures of the above handling robot, the working condition of the lifting system is relatively poor: its stiffness will determine whether the system can lift the workpiece and the positioning accuracy of the workpiece. In addition, considering the weight and geometric dimensions of the lifting system, it should not be designed too bulky. The scheme in Figure 1 adopts truss structure and parallel mechanism. However, the traditional method based on material mechanics cannot be applied for such complex spatial structure. With the development of finite element method (FEM) and the popularization of computer applications, the application of FEM to simulate complex mechanical structures has received research attentions [1-7]. Relative research on the applications of the finite element method on such case have seldom been reported and some research papers put more emphasis or attentions on the analysis of construction machinery [8-11]. For the lifting system of the AGV based robot in this research, it has its distinct characters and therefore the analysis results of stress and deformation are different with other cases. For such complex problem, the whole structure shall be reasonably simplified to reduce the computational burden as well as reflect the mechanical nature of the problem. In this paper, the finite element analysis of the lifting system of feed receiver disassembly and handling robot is performed using ABAQUS software to obtain the corresponding stress, strain and deformation results as well as provide reference for designers the actual working performance of the mechanism.

\* 594345789@qq.com

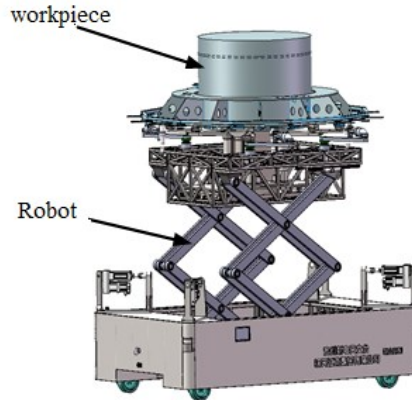


Figure 1. The AGV based robot.

## 2. THE CHARACTERS OF THE LIFTING SYSTEM

Figures 2 and 3 show the unilateral lifting part and bearing part of the lifting system. One end of the lower end of the lifting part is fixed, and the other end can move along the guide rail. Two extreme working conditions correspond to the cases where the lifting part are at the top and bottom respectively. When the two groups of lifting parts shrink or expand at the same time, it will drive the top to rise or fall. In order to reduce the weight, the bearing part is welded by hollow profile, and it can be considered as a truss structure. The advantage is clear: the structural rigidity can be ensured while the weight of the whole device is reduced. Both sides of the bottom of the bearing part of the lifting system are respectively consolidated with the upper end of the lifting part; the other end is connected through the guide rail, such that the upper end of the lifting part can move horizontally along the guide rail. Large deformations of the whole lifting system concentrate mainly on the bearing part and the lifting part. One side of the lifting part is hinged by 8 rods together with bearings. The rods adopt hollow structure except for the positions of both ends and central bearing holes. when the lifting mechanism is just unfolded, due to the geometric position relationship, the stiffness is small; this will result in large deformations or deflections at the top part.

All loads caused by the workpiece are applied to the bearing part. The upper part of the lifting part is connected with the lower part of the bearing part by the guide rail pair. Therefore, when the rod is unfolded, the horizontal degree of freedom of the lifting part can be ensured and more importantly, this can raise the bearing part. Due to the slow speed of the lifting part, it is not necessary to analyze the stress and the displacement of each situation; only the case where the truss structure is completely expanded is needed to be analyzed since this is the most complex situation of the lifting part and dangerous stress or displacement may appear.

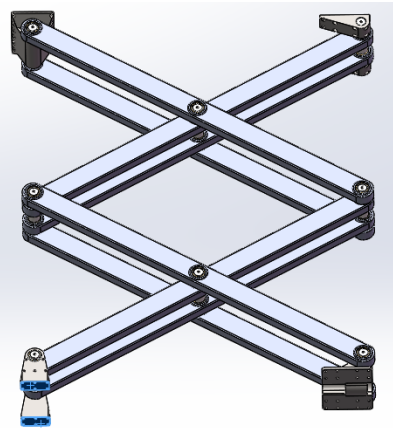


Figure 2. The lifting part of the lifting system.

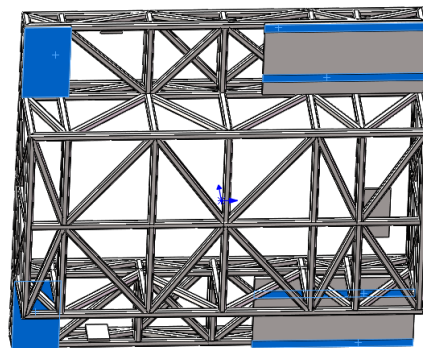


Figure 3. The bearing part of the lifting system.

### 3. FINITE ELEMENT ANALYSIS OF THE LIFTING SYSTEM

#### 3.1 Main ideas and work flow

Static analysis methods can be divided into two types: linear static analysis and nonlinear static analysis. Since there is no material nonlinearity and contact issues, performing linear static analysis is enough. By reasonable simplifications of the real-life problem in linear static analysis, analysis and computation efforts can be reduced. In this research, the Abaqus finite element analysis software is adopted and the main work flow includes: importing geometric model, assigning material properties, meshing and selecting the element type, assembling all the parts into a finite element model, setting analysis steps, applying loads and boundary conditions for the model, performing the computation, and acquiring the results.

Figure 4 presents the final finite element model in Abaqus. This research mainly focuses on the analysis of stress and deformations of the lifting system and the model is appropriately simplified according to the actual situations. For instance, the bearings at the connecting part of the lifting structure are replaced with the “Hinge” function in multi-body module of Abaqus. Meanwhile, the welding positions between mechanism and frame are considered as fixed boundary conditions.

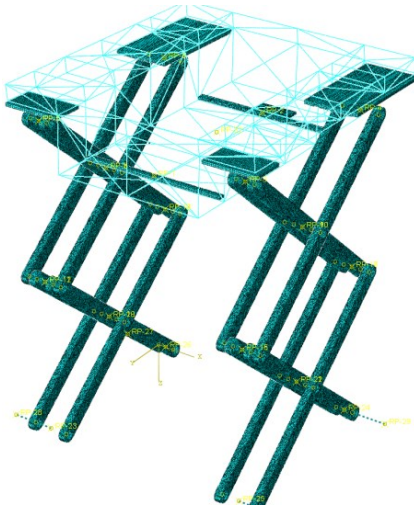


Figure 4. The finite element model.

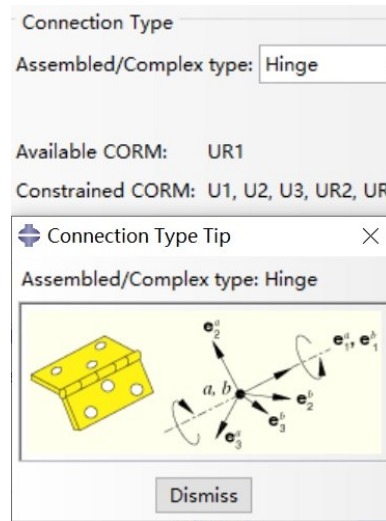


Figure 5. The “hinge” constraint.

#### 3.2 Finite element model with meshing

The bearing part of the whole lifting system can be deemed as a frame; since the size of the transverse section is smaller than the axial dimension, the profiles that form the frame can be simulated by beam elements. More specific, the quadratic beam elements are applied in this case because there is no contact problem or issues. There are two steel plates and guide rails at the bottom of the bracket on both sides. The steel plates and guide rails are welded with the bracket. Due to similar restricted degrees of freedom, the welded connection can thus be simulated with “coupling” constraint in building the finite element model. Similarly, the steel plates and guide rails at the upper part of the lifting structure and the lower part of the bracket can also be fixed by using coupling constraints in Abaqus. When the steel plates and guide rails are meshed, the hexahedral elements can be adopted to improve the precision of computation. The “hinge” constraint, as illustrated in Figure 5, can be applied to render the rotational freedom at the bearing without considering the actual slight force and deformation of the bearing. From Figure 5, it is not difficult to perceived that only the rotational degrees of freedom along the  $e_1$  direction are not limited; this is consistent with the degree of freedom of the real-life installed bearing. The lifting part is composed of 16 rods, whose interior is hollow to reduce the dead load while the middle part near the bearing is solid. Such hybrid property of rods brings difficulty in meshing the model. In such a case, the tetrahedral elements, with strong adaptability to complex geometric boundaries, are considered. To avoid poor accuracy of linear tetrahedral elements, this research therefore adopts the quadratic tetrahedral element to improve the computational precision; moreover, the meshes are refined near the geometry with sudden changes such as circumference since the stress and deformation results will be much more consistent with the real-life situations with more elements.

Since the bearing part of the lifting system can be deemed as a frame, this part can thus be given section attributes, e.g., size and thickness, in the software. The beam element B32 is considered; axial deformations, bending deformations and torsional deformations are allowed in Abaqus using beam elements. ‘B32’ beam element is a quadratic Timoshenko beam element, and it is suitable for slender beams. In addition, since the whole bearing part is a frame structure, there are no possible frictions or cases of open thin-walled beams; therefore, there is no need to consider other types of beam elements. The rods of the lifting part are meshed into tetrahedral elements, which can fit the complex geometric boundary of the part; the ‘‘C3D10’’ elements in Abaqus are adopted to improve the accuracy since this is a kind of quadratic element. Other kinds of tetrahedron elements are not under consideration because there are no possible contact issues between any two parts and the computation is performed using Abaqus/Standard module.

### 3.3 Boundary conditions

Similar with other engineering problems, boundary conditions of the lifting system in this research can be divided into two categories: load boundary conditions and displacement boundary conditions. The aim is to obtain the stress and the displacement distributions of the whole lifting system with the loads shown in Figure 6, where the frame is lifted to the maximum height of 2.9 m and suffers the vertical concentrated force  $F=50\text{ kN}$  as well as an interference torque  $T=189\text{ Nm}$  caused by the reaction force of on four corners of the frame. A reference point is then added at the bottom center of the frame as well as coupling constraints between the reference point and corresponding region; the loads can then be added at the reference point.

One side of the rods of the lifting part should be fixed when they drive the frame and the other side of them move horizontally and are driven by the screw and the servo motor. In such a case, the bottom of the rods of the lifting part moves close to each other and finally to raise the frame. The servo motor will stop when the frame is lifted at the specified height. Therefore, one side of the bottom rods should be fixed and this can be realized by placing fixed boundary conditions at appropriate locations to limit all degrees of freedoms. After applying all the boundary conditions the computations can be performed.

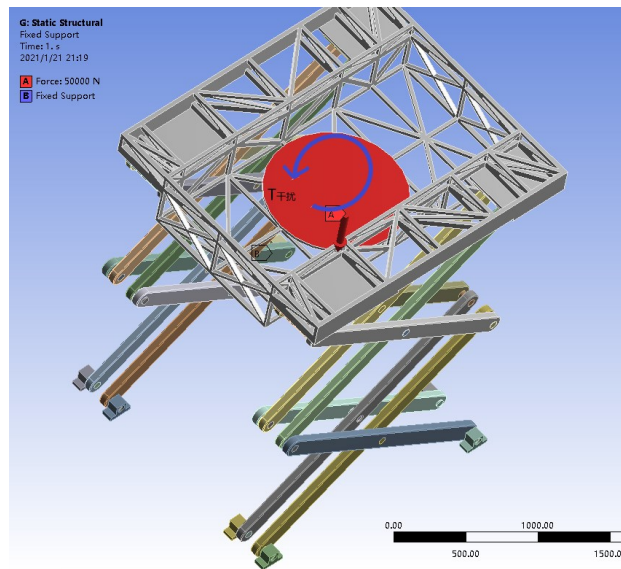


Figure 6. The loads applied on the frame.

## 4. RESULTS WITH DISCUSSIONS

All the analysis and computations are performed in Abaqus/standard module. Analysis steps are introduced in Abaqus to complete the analysis; all the boundary conditions and other setups can be specified in a step and this makes the analysis process easier to converge to the exact solution. In addition, the simulation or analysis of multi-loads and multi-procedures problems can also be simulated by setting analysis steps.

According to the strength theory, when the stress of a component at a certain place reaches the yield strength of the

material, e.g.,  $\sigma_s$ , plastic deformation will occur and the parts will have permanent deformation. The lifting system in this research is under great stress and its structural strength should be ensured first. The stress is not allowed to be greater than the material yield strength at any position of the whole lifting system studied in this paper. It should be noted that, the lifting system studied in this research has been preliminarily optimized in early stage; the main stress parts have been strengthened. Based on the fourth strength theory, the Mises stress value is taken as the equivalent stress value of the stress at any part of a part, and therefore, if the inequality  $\sigma \leq \bar{\sigma} = \left\{ 0.5 \cdot [(\sigma_1 - \sigma_2)^2 + (\sigma_2 - \sigma_3)^2 + (\sigma_3 - \sigma_1)^2] \right\}^{1/2}$  holds, it means that the stress at this place is safe and there is no possible plastic deformation. If the actual stress is less than the Mises stress value anywhere, the whole lifting system is safe. Q390B steel with yield strength of 410 MPa is used for the bearing part of the lifting system, and 45 steel with yield strength of 355 MPa is used for the rest. The Young's modulus is set to 210 MPa and Poisson's ratio is set to 0.3. According to technical requirements, the maximum deformation of the whole device shall not be greater than 20 mm. After adding the loads and constraints, the typical dangerous conditions, e.g., the frame of the bearing part is lifted to the highest place, are analyzed.

The resultant stress distribution is presented in Figure 7. Due to the position where the loads are added, the maximum stress of the whole system appears at the center of the bracket; the maximum stress is about 356 MPa, and it does not exceed the yield stress 410 MPa. The whole frame is supported by two sets of lifting parts, and both of them share the whole loads. The stress of each set of lifting parts is smaller (according to Figure 7, the maximum stress value is less than 140 MPa). Also, we can find out that the maximum stress appears at the middle of the following rods; this means that these rods are under large stress. There are two stiffeners at both sides of the bottom of the frame; as a result, the stress and deformation on both sides of the bottom of the frame are smaller than that at the center.

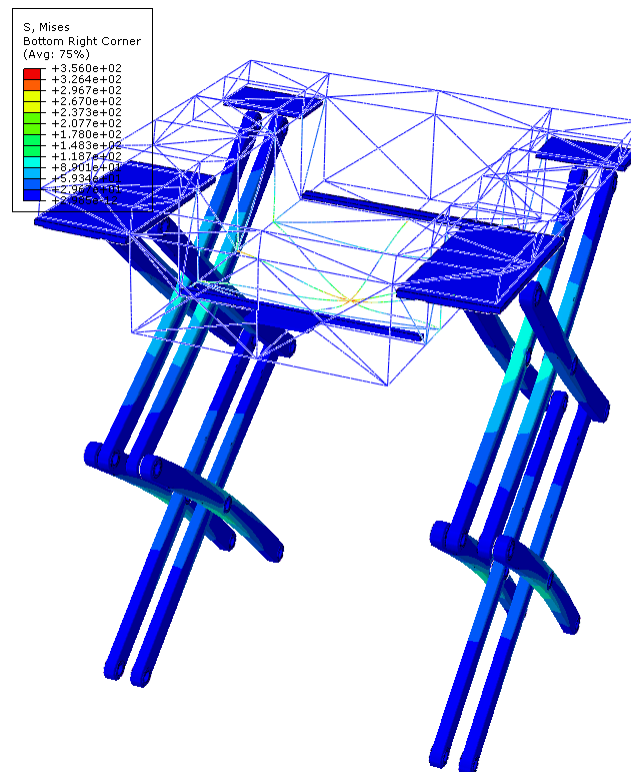


Figure 7. The stress distribution.

Figure 8 gives a deformation distribution diagram of the whole lifting system. Affected by the concentrated force at the bottom of the frame, the maximum deformation also occurs at the bottom of the frame. The maximum deformation is about 15 mm, which is within the allowable range. Affected by the position of the movable guide rail at the top of the lifting part, (different support positions), the deformation at the front and rear ends of the frame is somewhat different. For the lifting parts, due to the poor rigidity of the top, the deformation of the top rod is large; the rods at the bottom of

the lifting parts have good rigidity and small deformation. The actual deformation of the whole frame is not large except the middle part; the downward deformation of the whole bracket is caused by the deformation of several rods in the lifting parts.

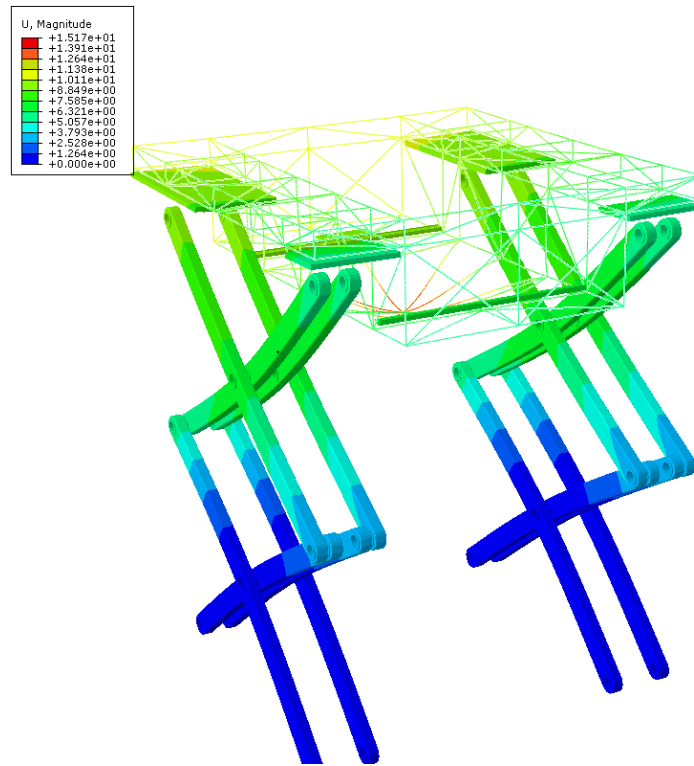


Figure 8. The deformation distribution.

## 5. CONCLUSIONS

In this research, the Abaqus finite element software is adopted to analyze the lifting system of the FAST receiver robot. with proper constraints to simplify the finite element model, mechanical essence of the model is reflected and the computational burden can also be reduced. After meshing the model, selecting element types, assigning loads and constraints, the deformation and stress results of the whole model have been obtained.

The results show that the maximum stress appears at the center of the frame, and the value is about 356 MPa; although the yield stress of the material is not exceeded, the bottom of the frame shall be strengthened. Large deformations appear at the bottom of the frame of the bearing part and the upper rod of the lifting part; the maximum deformation is about 15 mm, which is within the allowable tolerance. Based on the stress and the displacement results, the center of the frame and the rods of the lifting part can be further strengthened; for example, the layout of profiles at the bottom of the frame of the bearing part can be properly densified and the wall thickness of the rods can be increased.

## ACKNOWLEDGMENTS

This research is supported by the national key R & D plan (NO.2019YFB1312704).

## REFERENCES

- [1] An, J. S., Shi, J. J. and Gao, G. J., "Finite element analysis of ZY4000/09/19D hydraulic support," Coal Mine Machinery

- 42(2), 84-6 (2021).
- [2] He, S. L., "Finite element analysis of the segment lifting hanger," *Machinery Manufacturing* 57(5), 61-4 (2019).
  - [3] Saeed, T., Abbas, I. and Marin, M., "A GL model on thermo-elastic interaction in a poroelastic material using finite element method," *Symmetry* 12(3), 1-14 (2020).
  - [4] Giannaros, E., Kotzakolios, T. and Kostopoulos, V., "Blast response of composite pipeline structure using finite element techniques," *Journal of Composite Materials* 50(25), 3459-76 (2016).
  - [5] Zhang, J. J., Lu, G. X., Ruan, D. and Wang, Z. H., "Tensile behavior of an auxetic structure: Analytical modeling and finite element analysis," *International Journal of Mechanical Sciences* 136, 143-54 (2018).
  - [6] Sinegub, A. V. and Lopota, A. V., "Finite element analysis of a screw with cellular structure and bone thread for direct bone anchoring of prostheses," *Biomedical Engineering* 55(6), 425-8 (2022).
  - [7] Malta, E. R. and Martins, C. D. A., "Finite element analysis of flexible pipes under compression: A study on the damaged high strength tape and its effects on tensile armor instability," *Ocean Engineering* 245, 110470 (2022).
  - [8] Gan, S. L., Mei, Y., Yan, T. C. and Wu, Q., "Finite element analysis and structure optimum of flat-top tower cranes," *Modern Manufacturing Engineering* (3), 147-151+156 (2020).
  - [9] Zhou, Y. Q. and Zhou, Y. L., "Parametrization design method for key components of hydraulic support based on finite element," *Coal Mine Machinery* 41(12), 17-9 (2020).
  - [10] Zhai, G. D., Yang, X., Lu, X. H., Ji, R. J. and Hu, W. Y., "Finite element analysis of canopy column socket and column hinge joint of hydraulic support," *Coal Mine Machinery* 42(1), 64-6 (2021).
  - [11] He, L. T., "Finite element analysis and optimal design of the JS150 rotary drilling rig," *Machinery Manufacturing* 59(7), 41-43+55 (2021).